Jørgensen, B.B., D'Hondt, S.L., and Miller, D.J. (Eds.)
Proceedings of the Ocean Drilling Program, Scientific Results Volume 201

15. Data Report: Radiocarbon Dating and Sedimentation Rates for Holocene–Upper Pleistocene Sediments, Eastern Equatorial Pacific and Peru Continental Margin[1]

C. Gregory Skilbeck[2] and David Fink[3]

INTRODUCTION

As part of a wider paleoclimate and paleoceanographic study of Holocene–upper Pleistocene laminated sediments from the eastern equatorial Pacific and Peru continental margin, we completed 32 accelerator mass spectrometry (AMS) ^{14}C dates from cores recovered during Ocean Drilling Program (ODP) Leg 201. Sample preparation and measurement were carried out at the ANTARES AMS facility, Australian Nuclear Science and Technology Organisation (ANSTO), in Sydney, Australia (Lawson et al., 2000; Fink et al., 2004). Although the sediments are predominantly diatomaceous oozes (D'Hondt, Jørgensen, Miller, et al., 2003), they contain sufficient inorganic (e.g., foraminifer tests and nannofossil plates) and organic (**Meister et al.,** this volume) carbon to allow ^{14}C dating. These dates permitted us to reconstruct a history of sediment accumulation over the past 20 k.y., particularly on the Peru continental margin.

During previous ODP legs in the eastern equatorial Pacific (Leg 138; Mayer, Pisias, Janecek, et al., 1992) and the Peru continental margin (Leg 112; Suess, von Huene, et al., 1988), dating of upper Pleistocene–Holocene sections was determined by biostratigraphic study of several microfossil groups, including calcareous nannofossils, planktonic foraminifers, radiolarians, and diatoms. These studies only allowed division of the sections within a broad chronological range of ~100 k.y. in the

[1]Skilbeck, C.G., and Fink, D., 2006. Data report: Radiocarbon dating and sedimentation rates for Holocene–upper Pleistocene sediments, eastern equatorial Pacific and Peru continental margin. *In* Jørgensen, B.B., D'Hondt, S.L., and Miller, D.J. (Eds.), *Proc. ODP, Sci. Results,* 201, 1–15 [Online]. Available from World Wide Web: <http://www-odp.tamu.edu/publications/201_SR/VOLUME/CHAPTERS/108.PDF>. [Cited YYYY-MM-DD]
[2]Department of Environmental Sciences, University of Technology, Sydney NSW 2007, Australia.
g.skilbeck@uts.edu.au
[3]ANSTO-Environment, PMB 1, Menai NSW 2234, Australia.

Initial receipt: 23 July 2004
Acceptance: 19 March 2006
Web publication: 19 June 2006
Ms 201SR-108

Quaternary. More often than not, however, the uppermost parts of cores have been lumped together as "Quaternary" or "Holocene–Pleistocene" (Mayer, Pisias, Janecek, et al., 1992; Suess, von Huene, et al., 1988). Previous studies of sedimentary records off the coast of central Peru have employed radiocarbon dating. De Vries and Schrader (1981) undertook a study of the upwelling record through analysis of diatom taxonomy over the Holocene Marine Oxygen Isotope (MOI) Stage 2 deglaciation (from ~25 to 10 ka; also named the last glacial–interglacial transition [LGIT]), and their data suggest the presence of several localized unconformities throughout this part of the record. More recently, Rein et al. (2003) reported 42 AMS ^{14}C dates from the study of an 11-m core (106 KL) spanning the period from Last Glacial Maximum (LGM) to present from the vicinity of Sites 1228 and 1229.

In this report we present ^{14}C AMS dates and other pertinent data from cores from Sites 1227, 1228, and 1229 collected during Leg 201 at the Peru continental margin. The majority of these are either in correct stratigraphic order or, where this is not the case, within the 2σ range of adjacent dates. Regardless, groups of between five and six consecutive (with respect to depth) radiocarbon ages define consistent linear sedimentation rates with a high degree of confidence ($R^2 > 0.9$) for the late Holocene and part of the LGIT period. Fewer dates are available for the lower Holocene section, and these cannot be interpreted with confidence; however, they do suggest a significantly lower early Holocene sedimentation rate compared with either the late Holocene or the LGIT (MOI Stage 2) periods. Six radiocarbon ages from the stratigraphically deepest part of the section dated in Hole 1228B yielded late MOI Stage 3 ages ranging from 28,740 to 44,550 radiocarbon yr. The age-depth profile for these samples is not as well defined as those for the later periods cited above. With an R^2 approximately equal to 0.1 and inverse stratigraphic ordering, no conclusion can be made with respect to estimation of a reliable sedimentation rate. This could be a result of the very low total carbon contents of these samples (<3 wt%), which may lead to inconsistencies in extracting a uniform component of organic carbon during sample processing, inhomogeneity in carbon distribution in the sediment, and/or postdepositional alteration of carbon through the sample profile, which may invert stratigraphic control. The results, therefore, are not considered reliable enough to be used for further high-resolution studies. We obtained only single radiocarbon ages for sediment samples from the uppermost parts of the sedimentary section at Sites 1225, 1226, 1230, and 1231 for the reasons discussed below.

METHODS

In all cases, radiocarbon ages were obtained from the organic carbon fraction extracted from bulk sediment samples cut from 1-cm-thick sample slices taken from the sample half of the nominated core. Samples were pretreated with addition of dilute 2-M HCl for 3 hr at 60°C in order to remove any carbonate materials, including microfossils and detrital matter. The residue was then washed three times with water, dried, and combusted to convert all organic carbon to CO_2. The CO_2 was reduced to graphite by conventional means (Hua et al., 2001). All sample processing steps were carried out at ANSTO. AMS measurements were carried out at the ANSTO ANTARES AMS facility. All Holocene ^{14}C

dates were completed with radiocarbon age precision between 0.3% and 0.7% error (Fink et al., 2004).

The initial sample batch collected during Leg 201 (sample numbers OZG and OZF in Table T1) were shipped under frozen carbon dioxide from Valparaiso, Chile, to Sydney and then refrigerated until analysis. A second batch of samples (sample numbers OZH in Table T1) was dispatched from the Gulf Coast Core Repository at Texas A&M University (TAMU; USA) under ice and similarly refrigerated until analysis. Initially, a single sample from a depth between ~10 and 20 cm at each site was ^{14}C dated. For those yielding sedimentation rates of <5 cm/k.y., no further age dating was carried out, as the sedimentation rate was too low to allow subcentury resolution for geochemical, magnetic susceptibility, or reflected light study for paleoceanographic purposes. This resulted in solitary ^{14}C dates for uppermost sections (approximately <20 cm) at Sites 1225, 1226, 1230, and 1231. The stratigraphic position of these dated samples within each core and geographic core location are shown in Figure F1. Comprehensive dating of a core from each of the remaining three sites (1227, 1228, and 1229), all from the Peru continental margin, was then carried out. Sedimentation patterns and the stratigraphy defined by the dates are discussed in the following section.

T1. ^{14}C dates, p. 14.

F1. Leg 201 sites, p. 11.

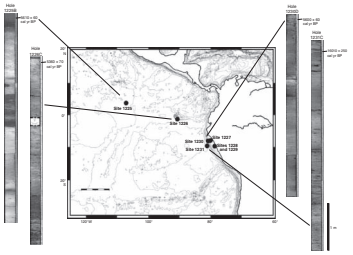

RESULTS

Conventional radiocarbon and calibrated ages are given in Table T1. Calibrations were carried out using the CALIB program (Stuiver and Reimer, 1993; v4.4.2) with the MARINE98 calibration curve. The local marine reservoir correction used was ΔR = 238 ± 49 (Marine Reservoir Correction Database [MRCD; radiocarbon.pa.qub.ac.uk/marine/; Reimer and Reimer, 2001, supplementary material at www.calib.org] Site 108 [Taylor and Berger, 1967]) for Sites 1227–1231 and ΔR = 58 ± 47 (MRCD Site 107) for Sites 1225 and 1226. We are aware that the ΔR corrections of Taylor and Berger (1967) have been obtained from coastal shell samples and so probably represent the ^{14}C reservoir effect of surface waters rather than that of the seabed. Given that deep waters usually have an older ^{14}C age than surface waters, our use of this ΔR correction should be considered as a minimum correction. Regardless of the age relative to present (AD 1950), application of a constant ΔR downcore will allow us to calculate sediment accumulation rates that can be reliably compared, unless there have been significant fluctuations in atmospheric radiometric carbon production over the accumulation interval.

For all dates that fall within the marine calibration range (i.e., those less than ~21 ka), with the exceptions of Samples 201-1228B-1H-2, 92–93 cm (OZG107); 60–61 cm (OZH149); and 179–80 cm (OZH150), the age quoted in Table T1 is the median probability age, and the error is plus or minus one-half of the second standard deviation range, which contains 100% of the probability distribution. For the three exceptions listed above, the error is plus or minus one-half of the first standard deviation range containing the largest proportion of the probability distribution, these being 73%, 82%, and 52%, respectively. All ages and errors have been rounded according to the conventions of Stuiver and Polach (1977). With one exception (the reversal of ages for Samples 201-1227B-1H-1, 26–27 cm, and 54–56 cm, which we consider to be equivalent within the 1σ error), all other ^{14}C ages obtained for the Holocene and LGIT core sections are in correct stratigraphic order.

The radiocarbon ages obtained in this study allow division of the stratigraphic section at the Peru continental margin sites into an uppermost Holocene section underlain by an upper Pleistocene (MOI Stages 2 and 3) interval, where both are present. As described below, these can be equated with subtle changes in the lithostratigraphy. They reveal that the Holocene is probably not present at Site 1227 but is represented by >2 m of core at both Sites 1228 and 1229.

STRATIGRAPHY

All core photographs shown in Figures F1 and F2 have been digitally contrast enhanced using Adobe Photoshop 7.0 to highlight visible lithostratigraphy. Although the actual contrast and brightness modification applied was different for each image, they were applied uniformly to each image individually, so that relative differences within each image are retained.

F2. Site stratigraphy, p. 12.

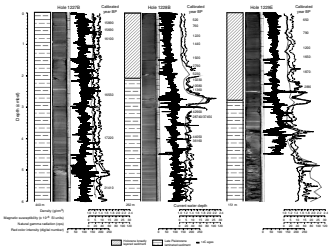

Single-Date Sites

Images of the four cores with single ^{14}C ages are shown in Figure F1. Detailed high-resolution chronological division of these sections is not possible, but examination of the single age dates and their relationship to the visible lithology suggests that decimeter-scale layering is present in the uppermost parts of at least three of the four images (representing the uppermost parts of Holes 1225B, 1226C, and 1230D). At Site 1225, the banding comprises alternations of paler and darker predominantly nannofossil ooze. The boundaries between the layers are gradational, and the layers themselves are mottled, indicating bioturbation (Shipboard Scientific Party, 2003a). At Sites 1226 and 1230, the cyclicity is of the same magnitude and style, comprising alternations of nannofossil (paler color) and diatom ooze, but a higher clay content, represented by the increase in greenish gray color in the sediments, is attributed to increasing proximity to the South American continent. The layering in cores from Site 1231 is similar to that at Sites 1226 and 1230, but there is a sharp curvilinear discontinuity at 27 cm below seafloor (cmbsf) separating mottled reddish brown sediments above from gray-green ooze below. We suspect this boundary represents an unconformity. A thin, 5-cm brownish layer is present at the top of Hole 1226B, but this unit has a gradational lower boundary and is more similar to the brownish gray layers in Hole 1225B that the Shipboard Scientific Party (2003a) described as containing Mn and iron oxides, attributed to redox processes.

Peru Margin Holocene

A 2.0- to 2.5-m Holocene section is present at Sites 1228 and 1229 (Fig. F2). Holocene sediments are absent at Site 1227. The sediments are nannofossil-bearing diatom oozes with subordinate quartz and clay (Shipboard Scientific Party, 2003b).

In both Holes 1228B and 1229E, the Holocene section is characterized by subtle, fine laminations at millimeter to submillimeter scale. The Holocene has an overall slightly darker olive green–gray color compared with underlying upper Pleistocene sediments. This subtle difference can be attributed to slightly higher total organic carbon (TOC) values in the Holocene section (**Meister et al.,** this volume; Watson, 2003), a slightly higher clay content, and a slightly lower carbonate per-

centage overall, although there are significantly different values between the pale and dark laminae for each of these components in both the Holocene and upper Pleistocene deglaciation sections.

Peru Margin Last Glacial–Interglacial Transition

Almost 6 m of latest Pleistocene deglaciation sediments are present in Hole 1227B (Fig. F2). These strata are finely laminated at millimeter to submillimeter scale with the laminations more obvious than in the overlying Holocene section. The increased visibility of the laminations is a result of increasing contrast between the darker and lighter layers, with the latter being overwhelmingly dominated by diatom frustules (Shipboard Scientific Party, 2003b). The upper Pleistocene section overall has a paler greenish gray color compared with the overlying Holocene section, with the boundary between the two being gradational at both Sites 1228 and 1229.

A much thinner LGIT section is present in Hole 1228B, represented by <50 cm of stratigraphic section, and we cannot discount the presence of an unconformity between 2.7 and 3.0 mbsf in Hole 1228B. Such unconformities or depositional hiatuses are common throughout the Quaternary section (De Vries and Schrader, 1981; Reinhardt et al., 2002), where they are attributed by the latter authors to variations in activity of the poleward moving undercurrent on the shelf. Late Pleistocene sediment older than the LGM (i.e., MOI Stage 3) is identical in composition and stratification to post-LGM sediments, and so it is not possible to distinguish them on lithostratigraphic grounds. We believe we can extrapolate the Holocene/Pleistocene boundary in Hole 1229E to 270 cmbsf, based on the lithostratigraphic criteria described above, but would not be confident in assigning post- and pre-LGM ages to the sediment beneath this level in the absence of radiocarbon ages.

SEDIMENTATION RATES

Single-Date Cores

Sedimentation rates determined for the equatorial upwelling (Sites 1225 and 1226), open-ocean (Site 1231), and Peru Trench (Site 1230) sites are based on single dates for depths <23 cmbsf and assume the seafloor at 0 cm to be 0 ka. Rates calculated for these sites are 1.8, 2.4, 1.5, and 2.0 cm/k.y., respectively (Table T2). These values fit well within the average sedimentation rate range determined by Hagelberg et al. (1995) for the 0- to 5-Ma sections of cores recovered from approximately the same sites during Leg 138 (Site 1225 at Site 851 and Site 1226 at Site 846). In these cases, the sequences were determined by gamma ray attenuation density data to be stratigraphically continuous, and the ages were yielded biostratigraphically. Overall, these sedimentation rates are also comparable with those from elsewhere in the equatorial eastern Pacific, such as the 2.5- to 5.0-cm/k.y. sedimentation rates reported by Lea et al. (2000) from the Cocos Ridge just north of the equatorial upwelling zone in the eastern Pacific.

T2. Sedimentation rate summary, p. 15.

Age-Depth Profiles for Peru Margin Cores

Sedimentation rates for the Peru margin sites have been calculated from linear regression fits to multiple data points where these are available (Fig. F3), and the results are summarized in Table T2.

F3. Sedimentation rates, p. 13.

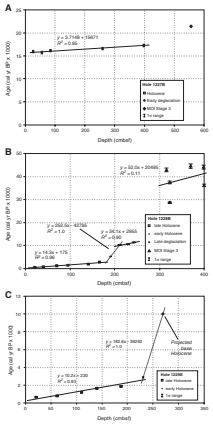

Hole 1227B

Holocene sediments are absent in Hole 1227B, with ~15.7 k.y. of sediment missing at the top of the hole. A continuous 1500-yr section defined by five radiocarbon ages is present below 26 cmbsf (Fig. F3A). This section spans the early part of the LGIT from ~15.7 to 17.2 ka. We estimate an accumulation rate of ~265 cm/k.y., nearly three times that of late Holocene. This period of extremely high sedimentation can probably be extended back to just prior to the LGM at ~21.5 ka.

Holes 1228B and 1229E

Well preserved upper Holocene sections are present at both Sites 1228 and 1229. At both they contain a sedimentation interval spanning 0 to ~2.8 ka that is characterized by sedimentation rates between 70 and 100 cm/k.y. (Fig. F3; Table T2). We are confident that in both Holes 1228B and 1229E a continuous section is present from the surface to ~2.8 ka.

In both Holes 1228B and 1229E the middle to early Holocene is represented by a much thinner stratigraphic section with fewer (Hole 1228B) or no (Hole 1229E) radiocarbon ages, and although we believe we can identify the base of the Holocene in the latter hole, we cannot be confident that unconformities are not present in this interval at both sites. Possible locations of breaks based on lithostratigraphic criteria are between 195 and 200 cmbsf in Hole 1228B and at ~250 cmbsf in Hole 1229E. With these possibilities in mind, average sediment accumulation rates over the middle–early Holocene were ~4–6 cm/k.y. at both sites.

A thin, 1000-yr duration deglaciation section at the Holocene/Pleistocene transition is present in Hole 1228B and is defined by three radiocarbon dates that yield a sedimentation rate of ~30 cm/k.y. (Table T2). This section can probably be extrapolated to ~270 cmbsf with a resultant age span increase of ~900 yr, from 10.2 to 12.2 ka.

The six late MOI Stage 3 radiocarbon ages from Hole 1228B (Fig. F3) do not represent a coherent data set for the reasons outlined above, and a repeat measurement on Sample 201-1228B-1H-3, 22–23 cm (OZG472 and OZH143), further exemplifies the problems where there is low residual modern carbon. Nevertheless, linear regression through these data points yields a sedimentation rate of ~20 cm/k.y., which is not incompatible with lithologically similar sediments from the uppermost Pleistocene deglaciation section in the same hole. We note, however, that the very high sedimentation rate early deglaciation section present in Hole 1227B is probably absent at these more southerly and shallower water sites.

DISCUSSION

Equatorial Pacific Upwelling, Peru Basin and Trench

Ages from the sites with single age dates (Site 1225, 1226, 1230, and 1231) suggest a typical oceanic pattern of precessional Milankovitch marine glacial–interglacial bedding (cf. Hodell, 1993) but with a clearly increasing terrestrial influence from west to east. Sediments are dominantly pelagic marine microfossil oozes but with variable amounts of clay and other terrestrial components. Sedimentation rates revealed by the ^{14}C dates are not considered unusual.

Peru Margin

The Peru continental margin is a shelf area dominated by upwelling and bottom-flowing countercurrents over at least the last 40 k.y. These currents prevent supply of oxygen to the bottom waters, as manifested by the absence of bioturbation and finely laminated sediments and additionally result in a number of localized sedimentation hiatuses or unconformities (De Vries and Schrader, 1981), particularly in water depths between 250 and 400 m (Reinhardt et al., 2002). The localized nature of unconformities is demonstrated by the absence of correlation between northernmost Site 1227 and southern Sites 1228 and 1229. In the north, Holocene and latest Pleistocene sediments are absent, and a well-developed late Pleistocene early deglaciation sequence accumulated at the considerable rate of 265 cm/k.y. for at least 1500 yr. The commencement of the rapid sedimentation at ~17.2 ka corresponds almost exactly with the onset of El Niño-Southern Oscillation activity proposed by Rein et al. (2003). The same time interval at Sites 1228 and 1229 is represented either by absent sections or very low sedimentation rates. Our interpretation is that initial melting of high-Andean glaciers after the LGM resulted in a flood of material and possibly nutrients to the shelf, but deposition on the shelf was not uniform at this time. Clearly, in some areas, particularly nearer the shoreline, sediment bypass or erosion took place.

In contrast, Holocene sedimentation is present at both Sites 1228 and 1229 but is absent from Site 1227. Within the Holocene, however, early to middle Holocene sedimentation (10.0–2.8 ka) was either very slow or missing. This observation corresponds with the findings of other authors that the Peruvian margin and hinterland was undergoing drought, at least during the period between 10.0 and 5 ka (Rein et al., 2003; Moy et al., 2002; Sandweiss et al., 1996), possibly as far back as 15.0 ka (Hebbeln et al., 2002). Most authors attribute this drought to the absence or reduction of El Niño during this period, resulting in much reduced precipitation along the northern South American hinterland.

The onset of more rapid sedimentation from 2.8 ka coincides with the timing of marked climate changes reported from Chile by Van Geel et al. (2000), which they interpreted to be a result of solar-induced changes to atmospheric circulation. At this stage, we cannot determine with confidence whether the high sedimentation rates along the Peru margin during the early part of deglaciation were enhanced by the onset of El Niño or were purely a result of glacial outwash, although Skilbeck et al. (2004) suggested the presence of El Niño cyclicity in these sediments. Our data do support a pattern whereby high sedimentation

rates existed from at least 17.2–15.7 ka, were reduced between ~12.0 and 2.8 ka, and then accelerated again over the past 2800 yr.

ACKNOWLEDGMENTS

Radiocarbon dates were made available through the Australian Institute of Nuclear Science and Engineering (AINSE), grants 02/169 and 04/139, and ANSTO-funded Project 0203V—cosmogenic Climate Archives in the Southern Hemisphere. Their support is gratefully acknowledged. We thank Ugo Zoppi and Quan Hua from ANSTO for sample preparation and measurement. We thank the ODP curatorial and core repository staff for supply of samples under request 17852A–D. This research used samples and data supplied by the Ocean Drilling Program (ODP). ODP is sponsored by the U.S. National Science Foundation (NSF) and participating countries under management of the Joint Oceanographic Institutions (JOI), Inc.

REFERENCES

De Vries, T.J., and Schrader, H., 1981. Variation of upwelling/oceanic conditions during the latest Pleistocene through Holocene off the central Peruvian coast: a diatom record. *Mar. Micropaleontol.,* 6(2):157–167. **doi:10.1016/0377-8398(81)90003-7**

D'Hondt, S., Jørgensen, B.B., Miller, D.J., et al., 2003. *Proc. ODP, Init. Repts.,* 201 [CD-ROM]. Available from: Ocean Drilling Program, Texas A&M University, College Station TX 77845-9547, USA. [**HTML**]

Fink, D., Hotchkis, M., Hua, Q., Jacobsen, G., Smith, A.M., Zoppi, U., Child, D., Mifsud, C., van der Gaast, H., Williams, A., and Williams, M., 2004. The ANTARES AMS facility at ANSTO. *Nucl. Instrum. Methods Phys. Res., Sect. B,* 224:109–115.

Hagelberg, T.K., Pisias, N.G., Shackleton, N.J., Mix, A.C., and Harris, S., 1995. Refinement of a high-resolution, continuous sedimentary section for studying equatorial Pacific Ocean paleoceanography, Leg 138. *In* Pisias, N.G., Mayer, L.A., Janecek, T.R., Palmer-Julson, A., and van Andel, T.H. (Eds.), *Proc. ODP, Sci Results,* 138: College Station, TX (Ocean Drilling Program), 31–46.

Hebbeln, D., Marchant, M., and Wefer, G., 2002. Paleoproductivity in the southern Peru–Chile Current through the last 33,000 years. *Mar. Geol.,* 186:487–504. **doi:10.1016/S0025-3227(02)00331-6**

Hodell, D.A., 1993. Late Pleistocene paleoceanography of the South Atlantic sector of the Southern Ocean: Ocean Drilling Program Hole 704A. *Paleoceanography,* 8:47–67.

Hua, Q., Jacobsen, G.E., Zoppi, U., Lawson, E.M., Williams, A.A., Smith, A.M., and McGann, M.J., 2001. Progress in radiocarbon target preparation at the ANTARES AMS centre. *Radiocarbon,* 43(2A):275–282.

Lawson, E.M., Elliot, G., Fallon, J., Fink, D., Hotchkis, M.A.C., Hua, Q., Jacobsen, G.E., Lee, P., Smith, A.M., Tuniz, C., and Zoppi, U., 2000. AMS at ANTARES—the first 10 years. *Nucl. Instrum. Methods Phys. Res., Sect. B,* 172:95–9.

Lea, D.W., Pak, D.K., and Spero, H.J., 2000. Climate impact of late Quaternary equatorial Pacific sea surface temperature variations. *Science,* 289:1719–1724. **doi:10.1126/science.289.5485.1719**

Mayer, L., Pisias, N., Janecek, T., et al., 1992. *Proc. ODP, Init. Repts.,* 138 (Pts. 1 and 2): College Station, TX (Ocean Drilling Program).

Moy, C.M., Seltzer, G.O., Rodbell, D.T., and Anderson, D.M., 2002. Variability of El Niño/southern oscillation activity at millennial timescales during the Holocene epoch. *Nature (London, U. K.),* 420:162–165. **doi:10.1038/nature01194**

Reimer, P.J., and Reimer, R.W., 2001. A marine reservoir correction database and online interface. *Radiocarbon,* 43:461–463.

Rein, B., Lückge, A., and Sirocko, F., 2003. A 20,000 year record of ENSO activity phases in Peru. *Geophys. Res. Abs.,* 5(01872).

Reinhardt, L., Kudrass, H.-R., Lückge, A., Wiedicke, M., Wunderlich, J., and Wendt, G., 2002. High-resolution sediment echosounding off Peru: late Quaternary depositional sequences and sedimentary structures of a current-dominated shelf. *Mar. Geophys. Res.,* 23:335–351. **doi:10.1023/A:1025781631558**

Sandweiss, D.H., Richardson, J.B., III, Reitz, E.J., Rollins, H.B., and Maasch, K.A., 1996. Geoarchaeological evidence from Peru for a 5000 years B.P. onset of El Niño. *Science,* 273:1531–1533.

Shipboard Scientific Party, 2003a. Site 1225. *In* D'Hondt, S.L., Jørgensen, B.B., Miller, D.J., et al., *Proc. ODP, Init. Repts.,* 201, 1–86 [CD-ROM]. Available from: Ocean Drilling Program, Texas A&M University, College Station TX 77845-9547, USA. [**HTML**]

Shipboard Scientific Party, 2003b. Site 1227. *In* D'Hondt, S.L., Jørgensen, B.B., Miller, D.J., et al., *Proc. ODP, Init. Repts.,* 201, 1–66 [CD-ROM]. Available from: Ocean Drilling Program, Texas A&M University, College Station TX 77845-9547, USA. [**HTML**]

Skilbeck, C.G, Goodwin, I, Gagan, M., Watson, M., and Aiello, I. 2004. High resolution palaeo-El Niño records from the Peru continental margin. *Proc. Int. Geol. Congr.,* 32(2):1033.

Stuiver, M., and Polach, H.A., 1977. Discussion and reporting of ^{14}C data. *Radiocarbon,* 19:355–363.

Stuiver, M., and Reimer, P.J., 1993. Extended ^{14}C database and revised CALIB 3.0 ^{14}C age calibration. *Radiocarbon,* 35:215–230.

Suess, E., von Huene, R., et al., 1988. *Proc. ODP, Init. Repts.,* 112: College Station, TX (Ocean Drilling Program).

Taylor, R.E., and Berger, R., 1967. Radiocarbon content of marine shells from the Pacific coasts of Central and South America. *Science,*158:1180–1182.

Van Geel, B., Heusser, C.J., Renssen, H., and Schuurmans, C.J.E., 2000. Climate change in Chile at around 2700 BP and global evidence for solar forcing: a hypothesis. *Holocene,* 10:659–664. **doi:10.1191/09596830094908**

Watson, M., 2003. The sedimentary record of ENSO in the eastern equatorial Pacific Ocean and Peru continental margin [B.Sc. thesis]. Univ. Technology, Sydney.

Figure F1. Location of sites drilled during Leg 201. Core photographs show the uppermost parts of the stratigraphic sequence at the four sites for which single ^{14}C dates were obtained. Radiocarbon ages shown adjacent to the columns are in calibrated year before present (cal yr BP) (see Table T1, p. 14, for details). Core images have been digitally contrast enhanced to highlight layering.

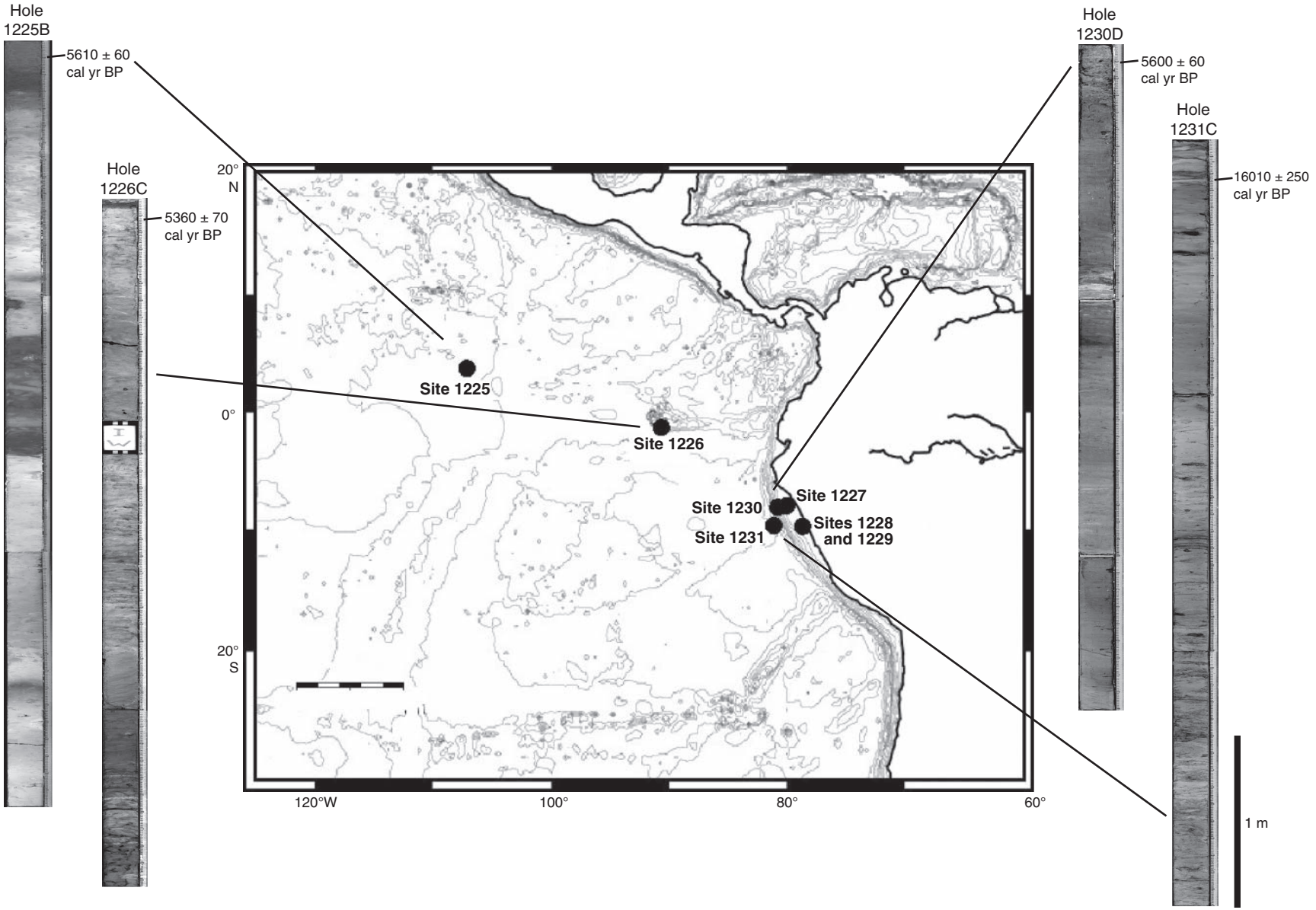

Figure F2. Holocene–late Pleistocene stratigraphy for Peru continental margin sites drilled during Leg 201. Radiocarbon dates obtained from bulk sediment analysis over 1-cm intervals. Core images have been digitally contrast enhanced to highlight laminations. Density, magnetic susceptibility, and natural gamma radiation geophysical logs were collected by the multisensor core logger, and red color intensity data were obtained from the high-resolution scanner, both deployed on the *JOIDES Resolution*. BP = before present.

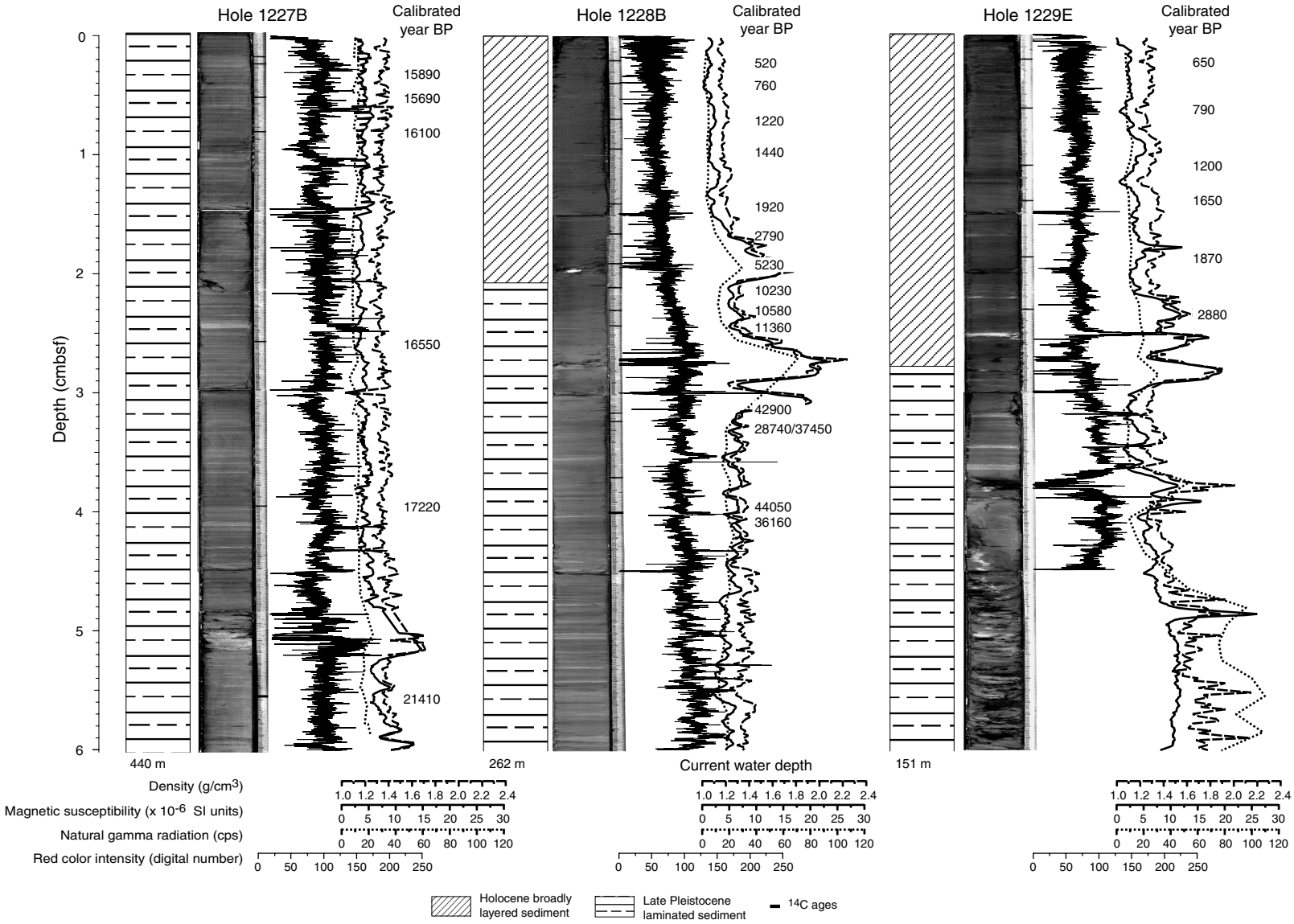

Figure F3. Sedimentation rates for Peru margin Sites (**A**) 1227, (**B**) 1228, and (**C**) 1229. Projected base of Holocene shown in C was determined from lithostratigraphy (see Fig. F2, p. 12). Regression coefficients of 1.0 indicate only two dates used. MOI = Marine Oxygen Isotope, cal yr BP = calibrated year before present.

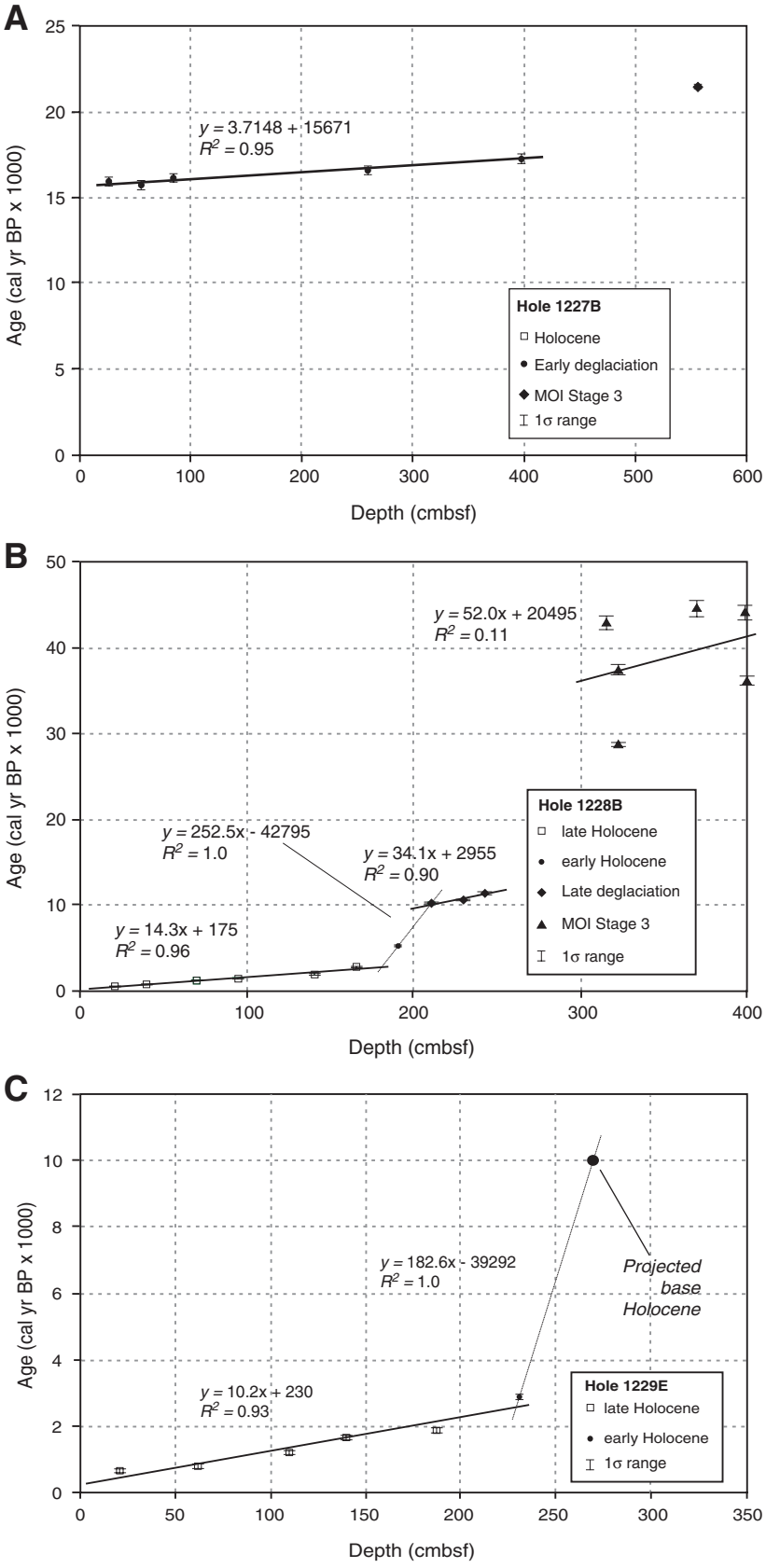

Table T1. Conventional and calibrated ^{14}C dates.

Core, section, interval (cm)	Laboratory code	Conventional ^{14}C date (yr BP)	1σ error	Calibrated ^{14}C date (cal yr BP)	1σ error	$\delta^{13}C$ (‰)	Depth (cmbsf)	Geographic location
201-1225B-								
1H-1, 9–10	OZF998	5,310	43	5,610	60	–20.7	9	2°46′N, 110°34′W
201-1226C-								
1H-1, 12–13	OZG004	5,064	44	5,360	70	–21	12	3°6′S, 90°49′W
201-1227B-								
1H-1, 26–27	OZG474	13,956	84	15,890	250	–21.0*	26	8°59′S, 79°57′W
1H-1, 54–56	OZG475	13,796	78	15,690	270	–21.0*	55	8°59′S, 79°57′W
1H-1, 84–85	OZG105	14,141	67	16,100	240	–21.0*	84	8°59′S, 79°57′W
1H-2, 109–110	OZG104	14,528	75	16,550	250	–20.3	259	8°59′S, 79°57′W
1H-3, 97–98	OZG103	15,103	107	17,220	280	–21.0*	397	8°59′S, 79°57′W
2H-1, 55–57	OZG106	21,439	122	21,410	130	–21.7	556	8°59′S, 79°57′W
201-1228B-								
1H-1, 20–21	OZG001	1,142	39	520	50	–21.0*	20	11°4′S, 78°5′W
1H-1, 39–40	OZH144	1,449	50	760	70	–20.1	39	11°4′S, 78°5′W
1H-1, 69–70	OZH145	1,902	35	1,220	50	–20.8	69	11°4′S, 78°5′W
1H-1, 94–95	OZH146	2,134	36	1,440	70	–20.9	94	11°4′S, 78°5′W
1H-1, 140–141	OZH147	2,550	36	1,920	70	–20.3	140	11°4′S, 78°5′W
1H-2, 15–16	OZH148	3,251	45	2,790	60	–21.0*	165	11°4′S, 78°5′W
1H-2, 40–41	OZG109	5,151	40	5,230	100	–21.6	190	11°4′S, 78°5′W
1H-2, 60–61	OZH149	9,793	50	10,230	130	–21.5	210	11°4′S, 78°5′W
1H-2, 79–80	OZH150	10,042	82	10,580	90	–19.7	229	11°4′S, 78°5′W
1H-2, 92–93	OZG107	10,648	58	11,360	170	–21.7	242	11°4′S, 78°5′W
1H-3, 15–16	OZH151	42,879	760	42,900	800	–21.3	315	11°4′S, 78°5′W
1H-3, 22–23	OZG472	28,779	251	28,740	250	–20.5	322	11°4′S, 78°5′W
1H-3, 22–23†	OZH143	37,446	599	37,450	600	–21.0*	322	11°4′S, 78°5′W
1H-3, 69–70	OZH152	44,554	935	44,550	950	–20.5	369	11°4′S, 78°5′W
1H-3, 98–99	OZH153	44,095	883	44,050	900	–21.3	398	11°4′S, 78°5′W
1H-3, 99–100	OZG473	36,156	514	36,160	520	–21.0*	399	11°4′S, 78°5′W
201-1229E-								
1H-1, 20–21	OZG002	1,331	42	650	60	–21.0*	20	10°59′S, 77°57′W
1H-1, 61–62	OZH154	1,484	35	790	70	–20.3	61	10°59′S, 77°57′W
1H-1, 109–110	OZG108	1,884	30	1,200	60	–20.8	109	10°59′S, 77°57′W
1H-1, 139–140	OZH155	2,313	32	1,650	70	–20.5	139	10°59′S, 77°57′W
1H-2, 36–37	OZH156	2,501	49	1,870	80	–21.3	186	10°59′S, 77°57′W
1H-2, 80–81	OZH157	3,348	42	2,880	80	–20.7	230	10°59′S, 77°57′W
201-1230D-								
1H-1, 10–11	OZG003	5,478	40	5,600	60	–23.4	10	9°7′S, 80°35′W
201-1231C-								
1H-1, 23–24	OZG005	14,059	89	16,010	250	–21.5	23	12°1′S, 81°54′W

Notes: All analyses were carried out at the ANSTO ANTARES AMS laboratory at Lucas Heights in Sydney, Australia, on bulk marine sediment samples and calculated using $\delta^{13}C$ relative to Peedee belemnite as shown. Calibrations were carried out using the CALIB program (Stuiver and Reimer, 1993; v4.4.2) with the MARINE98 calibration curve. The local marine reservoir correction in all cases is $\Delta R = 238 \pm 49$, with the exception of Sites 1225 and 1226, where a value of $\Delta R = 58 \pm 47$ was used. Conventional radiocarbon ages and errors are unrounded. Rounding of calibrated ages was carried out according to the protocols of Stuiver and Polach (1977). BP = before present, * = assumed values, † = repeat measurement on adjacent sample from same depth in core.

Table T2. Summary of sediment accumulation rates determined using ^{14}C chronology.

Hole	Depth (cmbsf)	Geological period	Correlation coefficient (R^2)	Sediment accumulation rate (cm/k.y.)
1225B	0–10	Holocene	—	*1.8*
1226B	0–13	Holocene	—	*2.4*
1227B	0–21	latest Holocene	—	*116.7*
	26–398	Late last deglaciation	0.95	266.8
1228B	0–21	latest Holocene	—	*40.4*
	20–166	late Holocene	0.96	70.1
	190–211	early–middle Holocene	—	*4*
	210–243	Late last deglaciation	0.9	29.3
	315–400	Late MOI Stage 3	0.11	19.2
1229E	0–21	latest Holocene	—	*32.3*
	20–231	late Holocene	0.93	98.1
	230–270	early–middle Holocene	—	*5.1*
1230D	0–11	Holocene	—	*2*
1231C	0–24	Holocene–late last deglaciation	—	*1.5*

Notes: Rates shown in italics are based on two dates only. In some cases, one of the dates is assumed, either seafloor age of 0 yr or base Holocene in Hole 1229E. — = coefficient not used.